The EMBO Journal vol.15 no.10 pp.2323–2330, 1996

A left-handed β-helix revealed by the crystal structure of a carbonic anhydrase from the archaeon *Methanosarcina thermophila*

Caroline Kisker, Hermann Schindelin, Birgit E.Alber[1], James G.Ferry[1] and Douglas C.Rees[2]

Division of Chemistry and Chemical Engineering, 147-75CH, California Institute of Technology, Pasadena, CA 91125 and [1]Department of Biochemistry and Molecular Biology, Pennsylvania State University, University Park, PA 16802-4500, USA

[2]Corresponding author

A carbonic anhydrase from the thermophilic archaeon *Methanosarcina thermophila* that exhibits no significant sequence similarity to known carbonic anhydrases has recently been characterized. Here we present the structure of this enzyme, which adopts a left-handed parallel β-helix fold. This fold is of particular interest since it contains only left-handed crossover connections between the parallel β-strands, which so far have been observed very infrequently. The active form of the enzyme is a trimer with three zinc-containing active sites, each located at the interface between two monomers. While the arrangement of active site groups differs between this enzyme and the carbonic anhydrases from higher vertebrates, there are structural similarities in the zinc coordination environment, suggestive of convergent evolution dictated by the chemical requirements for catalysis of the same reaction. Based on sequence similarities, the structure of this enzyme is the prototype of a new class of carbonic anhydrases with representatives in all three phylogenetic domains of life.

Keywords: archaea/carbonic anhydrase/convergent evolution/left-handed β-helix

Introduction

Carbonic anhydrases are Zn^{2+}-containing enzymes catalyzing the reversible hydration of CO_2. These metalloenzymes are among the fastest enzymes described so far (Lindskog, 1983) having turnover numbers of up to 10^6/s. They are widely distributed in nature and, until recently, two classes of carbonic anhydrases have been recognized (Fukuzawa *et al.*, 1992): the 'eukaryotic' class including seven isozymes from various higher vertebrates and two isozymes from *Chlamydomonas reinhardtii*, and the 'prokaryotic' class represented by chloroplast carbonic anhydrases and two bacterial enzymes. These enzymes participate in a variety of cellular functions (Sly and Hu, 1995), such as the transfer and accumulation of H^+ and HCO_3^-, pH homeostasis and ion transport.

When the methanogenic archaeon *Methanosarcina thermophila* is shifted from methanol to acetate as the energy source, the organism expresses a carbonic anhydrase (Cam). The sequence of Cam has no significant identity to all other carbonic anhydrases, suggesting the existence of a new class of these enzymes (Alber and Ferry, 1994). The amino acid sequence deduced from the gene indicates a signal peptide for Cam characteristic of an extracellular enzyme. Two possible metabolic roles for this carbonic anhydrase have been postulated, depending on its location. As a cytosolic enzyme, Cam could facilitate the uptake of acetate by supporting a CH_3COO^-/HCO_3^- antiport system. However, as an extracellular enzyme there are two possible functions: (i) support of a H^+/CH_3COO^- symport mechanism and/or (ii) conversion of CO_2 to HCO_3^- facilitating the removal of excess CO_2 produced by *M.thermophila* growing on acetate.

Since there is no significant sequence identity between Cam and the other two classes of carbonic anhydrases, we have solved the crystal structure of Cam in order to determine whether there are any common structural features either in the overall fold or in the active site architecture.

Results and discussion

The crystal structure of Cam was determined at 2.8 Å resolution (Tables I and II) using the method of multiple isomorphous replacement (MIR) in combination with 3-fold non-crystallographic symmetry (ncs) averaging and phase extension. The structure has been refined at 2.8 Å resolution to an *R*-factor of 0.235, resulting in a model of very good stereochemical quality (see Materials and methods).

Fold of the monomer

The polypeptide chain of Cam is characterized by a novel fold containing seven complete turns of a left-handed parallel β-helix (Figure 1A) which is topped by a short α-helix. A second α-helix formed by the C-terminal portion of the protein is positioned antiparallel to the axis of the β-helix. In addition, a short segment of the polypeptide chain at the N-terminus is in extended conformation. The cross-section of the β-helix resembles an equilateral triangle, as each turn of the β-helix contains three short β-strands of nearly equal length. As a consequence, the left-handed β-helix consists of three parallel sheets, which are essentially untwisted. Two of the three β-sheets contain seven strands each, whereas the third sheet has eight strands.

The basic length of one turn of the β-helix is 17 residues, but insertions of varying lengths are observed (Figure 1B). Each turn of the β-helix contains two type II β-turns, positioned between strands 1 and 2 and between strands 2 and 3, respectively, which are stabilized by H bonds between stacked β-turns (Figure 2A). These additional H bonds satisfy the main chain atom hydrogen bonding potential of residues i+1 and i+2 in each β-turn.

Table I. Data collection and multiple isomorphous replacement statistics

	NAT1	NAT2	PIP1	AU	PB	PIP2
d_{min} (Å)	3.17	2.8	3.5	3.5	3.5	3.17
Completeness	0.979	0.941	0.894	0.826	0.825	0.958
(Last shell)	(0.788)	(0.829)	(0.796)	(0.663)	(0.674)	(0.846)
Redundancy	3.9	3.2	2.6	3.5	2.9	4.6
(Last shell)	(3.2)	(2.6)	(2.3)	(3.3)	(2.8)	(4.0)
R_{sym}	0.088	0.064	0.109	0.085	0.101	0.096
(Last shell)	(0.267)	(0.324)	(0.360)	(0.238)	(0.255)	(0.359)
R_{deriv}	–	–	0.164	0.316	0.278	0.329
d_{min} (Å)	limit for MIR analysis		4.0	4.0	5.0	4.0
No. of sites	–	–	6	3	5	6
R_{Cullis}	–	–	0.53	0.83	0.92	0.90
Phasing power	–	–	1.53	0.91	0.55	0.73
FOM				0.483		

$R_{sym} = \Sigma_{hkl}\Sigma_i|I_i - \langle I\rangle|\Sigma_{hkl}\Sigma_i\langle I\rangle$ where I_i is the ith measurement and $\langle I\rangle$ is the weighted mean of all measurements of I.
$R_{deriv} = \Sigma_{hkl}||F_{PH}|-|F_P||/\Sigma_{hkl}|F_P|$ where F_P and F_{PH} are the native and heavy atom derivative structure factor amplitude.
$R_{Cullis} = \Sigma_{hkl}||F_{PH} \pm F_P| - |F_H||/\Sigma_{hkl}|F_{PH} - F_H|$ for centric reflections only, where F_H is the calculated heavy atom structure factor.
Phasing power is the mean value of the heavy atom structure factor amplitude divided by the residual lack of closure error.

This is different from a 'standard' β-turn where these atoms only form H bonds to nearby side chain atoms or solvent molecules. In the T1 turn, no H bonds are formed between residues i and i+3. However, polar side chain atoms of residues Ser72 and Thr131 form three-center H bonds with the main chain O of residue i and the main chain N of residue i+3 of the residues in the adjacent β-turn. As an example, the hydrogen bond interactions involving Ser72 are shown in Figure 2B. Each turn of the β-helix is completed by a loop connecting strand 3 with strand 1 of the next turn which is the only place where insertions in the core region of the β-helix seem to be tolerated.

The flat, untwisted nature of these sheets is reflected in the pronounced tendency for the main chain dihedral angles φ and ψ of residues in the β-sheets to have values of $\phi = -\psi$, in agreement with theoretical predictions (Schulz and Schirmer, 1979). The interior of the helix is completely dominated by hydrophobic interactions. Especially important seem to be stacking interactions between aliphatic side chains of residues originating from equivalent positions in adjacent turns of the helix (Figure 2C). In addition, there are also stacking interactions on the exterior of the helix involving both hydrophobic and hydrophilic side chains (not shown).

The trimer

The three molecules in the asymmetric unit form the active enzyme, a trimer with a 3-fold axis and approximate dimensions of 65×65×70 Å^3 (Figure 3A). An extensive area of the surface of each monomer participates in monomer–monomer interactions, with 2700 Å^2 of each monomer, or 25% of the molecular surface per subunit, buried upon trimerization. H bonds and salt bridges, as well as hydrophobic interactions, contribute to the stabilization of this interface. The side chain of Arg59 seems to be especially important, since it is forming salt bridges to Asp61 of the same monomer and Asp76 of another monomer. These three residues are almost entirely conserved in all proteins sharing homology with Cam (Figure 5), with only one type-conserved substitution of Asp76 by a glutamic acid. Asp61 also contacts Nε2 of His81, one of the Zn ligands, and all three residues are close to the active site.

Table II. Summary of crystallographic refinement of Cam

Resolution range (Å)	10.0–2.8
R_{cryst} all data/3 σ-cutoff	0.235/0.213
R_{free} all data/3 σ-cutoff	0.293/0.273
r.m.s. deviations in	
bond lengths (Å)	0.013
bond angles (°)	1.70
torsion angles (°)	27.04
improper torsion angles (°)	2.43

$R_{cryst} = \Sigma||F_o|-|F_c||/|F_o|$ where F_o and F_c are the observed and calculated structure factor amplitudes. R_{free} same as R_{cryst} for 5% of the data omitted from the refinement.

In the crystal, two trimers dimerize to form a hexamer with 32-symmetry, by association of the N-termini of the six monomers into a 6-stranded β-structure with a hydrophobic core (Figure 3B). The structure solution of the orthorhombic crystal form revealed the same hexamer, suggesting that its presence in the tetragonal crystal form is not due to crystal packing artefacts. It should be noted, however, that the additional methionine residue present in the cloned enzyme (see Materials and methods) is part of the trimer–trimer interaction and, thus, the association of two trimers to a hexamer might not be present in the wild-type enzyme. Analytical ultracentrifugation experiments (unpublished results) indicate that the trimer of Cam is the predominant form in solution.

Active site architecture

The most important aspect of the trimerization is the formation of Zn^{2+}-containing active sites at the subunit–subunit interfaces. Residues contributing to each of the three active sites originate from adjacent monomers (Figure 4A); the Zn^{2+} is coordinated by Nδ1 of His81 and Nε2 of His122, which extend from equivalent positions of adjacent turns of the β-helix of one monomer, by Nε2 of His117 located in the β-helix of the neighboring monomer and by a tentatively assigned water molecule resulting in a distorted tetrahedral geometry. This putative water molecule in turn is within hydrogen bonding distance

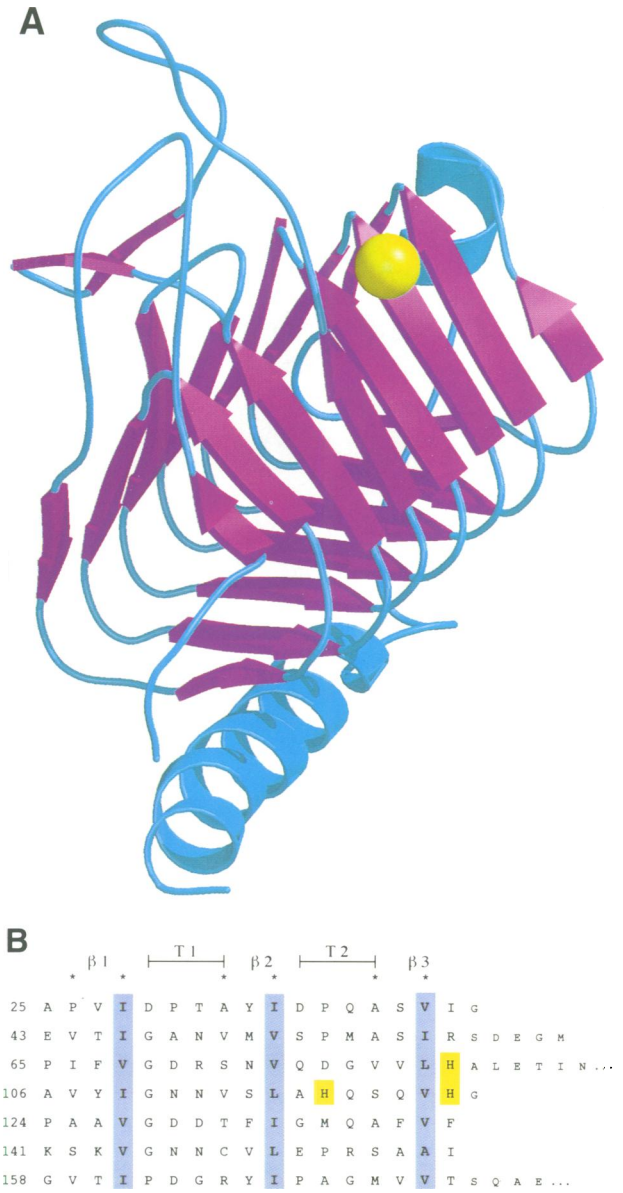

Fig. 1. (**A**) Side view of the Cam monomer. In this schematic drawing, β-strands are shown as curved arrows in purple and α-helices as ribbons in cyan. The active site Zn^{2+} ion is shown with its van der Waals surface in yellow. All representations of the structure were prepared using MOLSCRIPT (Kraulis, 1991) and RASTER3D (Bacon and Anderson, 1988). (**B**) Sequence alignment of the internal repeat of Cam showing residues pointing into the interior of the β-helix (*), type-conserved aliphatic side chains in blue, Zn^{2+} ligands in yellow, the location of residues in the two β-turns T1 and T2 and the three β-strands in each turn of the β-helix.

to Oε1 of Gln75. The shape of the electron density at the fourth Zn^{2+} coordination site (Figure 4B) does not support azide as the fourth ligand which is present in the crystallization solution and is an inhibitor of both Cam and the eukaryotic carbonic anhydrases. A more detailed description of the interactions near the active site has to await structure refinement at higher resolution, including studies with bound inhibitors.

The active site of Cam can be superimposed onto the corresponding residues of human carbonic anhydrase II (CBAII) using the Zn^{2+} ion and ligands as reference. All atoms of His81, the side chain atoms of His122, Nε2 of His117 and the Zn^{2+} have been used for the superposition, yielding a root mean square (r.m.s.) deviation of 0.84 Å. Coordinates of CBAII (Håkansson *et al.*, 1992) were taken from the PDB, entry code 2CBA. As seen in Figure 4C, the immediate Zn^{2+} coordination environment is similar in these two carbonic anhydrases. Remarkably, the coordination of the metal by the same N atoms of the imidazole rings is conserved, indicating convergent evolution of these active sites. In addition to the Zn^{2+} ligands, Glu62 and Gln75 of Cam are located close to the active site and may be the counterparts of Glu106 and Thr199 in CBA II. However, only Gln75 is conserved in the Cam family of proteins (Figure 5), whereas Glu106 and Thr199 are conserved in all carbonic anhydrases from higher vertebrates (Sly and Hu, 1995). The latter residues participate in a hydrogen bond network required for optimal catalytic activity of the Zn^{2+}-bound hydroxide (Xue *et al.*, 1993).

Right-handed versus left-handed β-helices

Parallel β-helices with three strands per turn have been observed only recently in the monomeric structures of three pectate lyases (Yoder *et al.*, 1993; Lietzke *et al.*, 1994; Pickersgill *et al.*, 1994) and in the trimeric phage P22 tail spike protein (Steinbacher *et al.*, 1994). In contrast to the structure of Cam, the β-helix in these proteins is right-handed. In addition to the opposite hand of the helix, there are other features (Yoder and Jurnak, 1995) that are different in comparison with Cam: the cross-section of the β-helices is kidney-shaped, there are at least 22 residues per turn, insertions occur between strands 1 and 2 as well as between strands 3 and 1, and the β-sheets also show the usually observed twist. In general, the β-helix core of Cam could be described as having a much more regular shape than the core of these proteins. Very recently, a left-handed β-helix has been discovered in the structure of UDP-*N*-acetylglucosamine acyltransferase (Raetz and Roderick, 1995). As in the β-helix of Cam, each turn resembles an equilateral triangle and comprises three short β-strands per turn. Each strand contributes two residues that project into the interior, with the second of these residues always being an aliphatic side chain, predominantly Val or Ile in both enzymes. In addition, UDP-*N*-acetylglucosamine acyltransferase also forms a trimer, but the association of the three monomers is somewhat different. Compared with Cam, each monomer appears to be rotated slightly around its central axis so that interactions between monomers only take place around one of the three turns next to the 3-fold axis. The location of the Zn^{2+} ion at the subunit interface, as well as the C-terminal α-helix, lead to more extensive monomer–monomer interactions in Cam.

As a consequence of the left-handed β-helix of Cam, all crossovers between neighboring strands are of the unusual left-handed type. Left-handed crossovers have been observed very infrequently, with isolated examples in subtilisin (Wright *et al.*, 1969), class 1 human leukocyte antigen (Bjorkman *et al.*, 1987), elongation factor-G (Ævarsson *et al.*, 1994) and two examples in KP4 toxin (Gu *et al.*, 1995). One possible explanation for the pronounced preference for right-handed crossovers between two parallel β-strands has been the right-handed local twist of an isolated β-strand (Richardson, 1976;

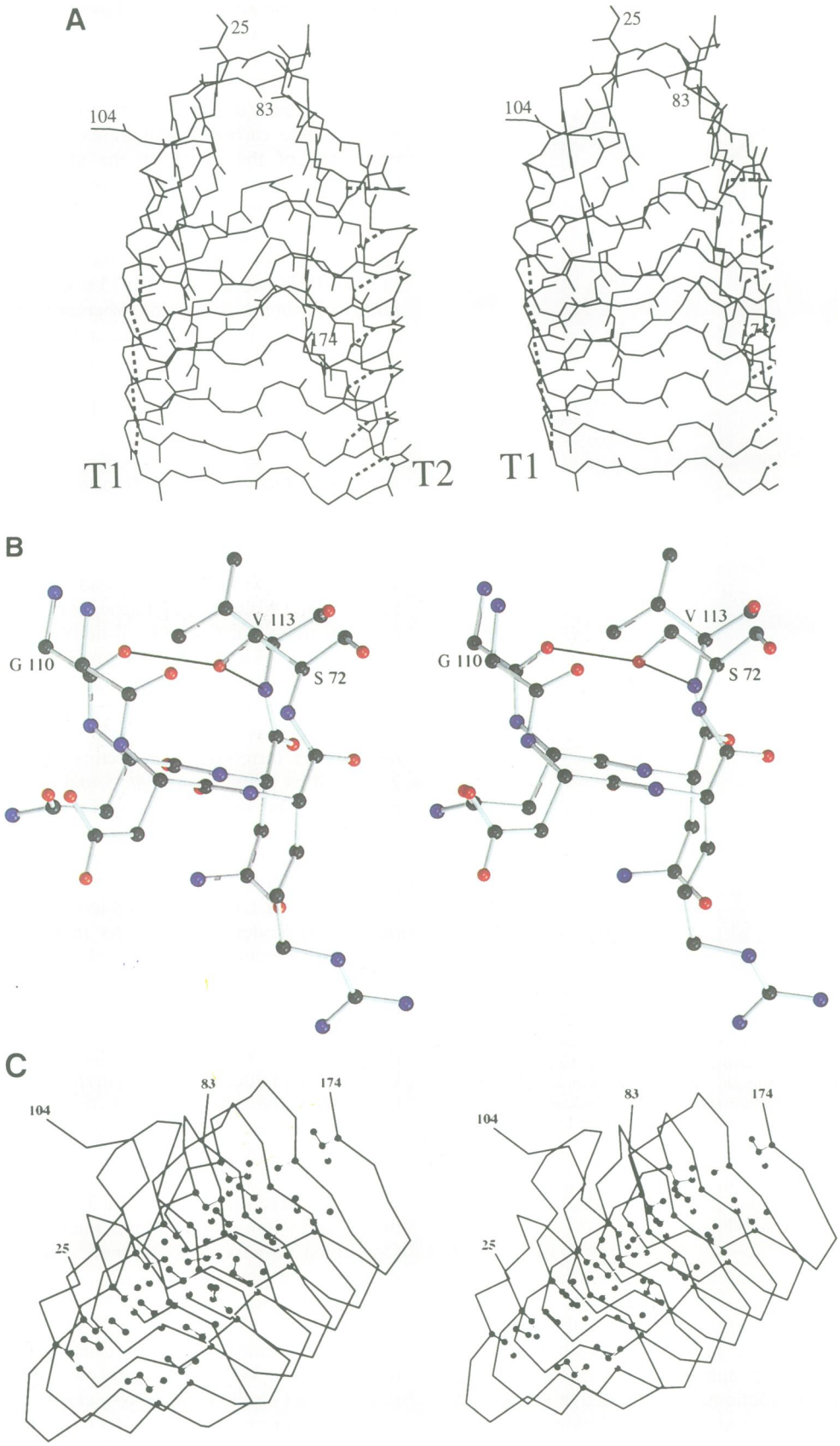

Fig. 2. (**A**) Stereo main chain drawing of the β-helix core showing H bonds (dashed lines) within and between adjacent turns T1 and T2. In the T1 turn, no H bonds are formed between residues i and i+3. (**B**) Three-center H bonds (black lines) involving Ser72, the main chain O of Gly110 and the main chain N of Val113 of the adjacent β-turn. (**C**) Cα-stereo drawing of the β-helix core with type-conserved aliphatic side chains pointing into the interior and stacked on top of each other.

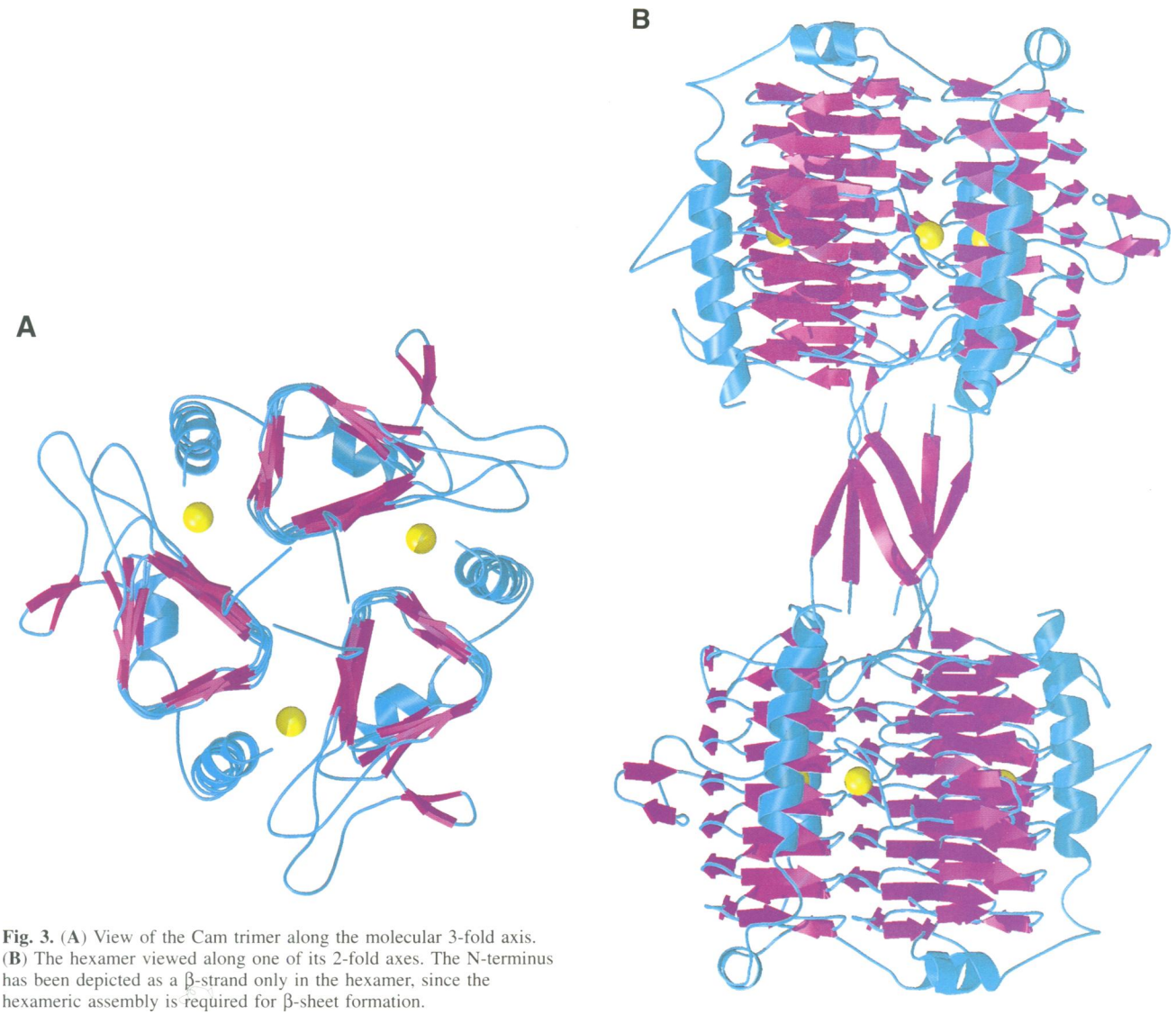

Fig. 3. (**A**) View of the Cam trimer along the molecular 3-fold axis. (**B**) The hexamer viewed along one of its 2-fold axes. The N-terminus has been depicted as a β-strand only in the hexamer, since the hexameric assembly is required for β-sheet formation.

Sternberg and Thornton, 1977), which leads to shorter connections for right-handed crossovers. Consistent with this explanation are the untwisted sheets in the β-helix of Cam and the twisted sheets of its right-handed counterparts.

Structural determinants of this fold

Which factors contribute to the formation of a left-handed β-helix in Cam? An examination of the backbone torsion angles reveals that in the core region all residues are in extended conformation, with the only exception being residues at positions i+2 of the T1 and T2 turns. As these latter residues have a conformation typically found in left-handed α-helices, they introduce a left-handed bend in the otherwise straight polypeptide chain. The occurrence of these residues at the i+2 positions is in agreement with statistical observations (Wilmot and Thornton, 1988) except for the low number of glycines, which might reflect the importance of side chain stacking interactions in this fold. Each turn of the β-helix is completed by a loop which either has one residue in a left-handed conformation (Lys141 and Gly158), a *cis*-proline (Pro124 and Pro65) or simply more residues in the longer loops to introduce the bend necessary for completion of one turn. The location of all these residues at critical positions in the pseudo-repetitive sequence seems to be a major factor for the observed left-handedness of the β-helix of Cam. Undoubtedly, there is also a cooperative effect during protein folding: once one left-handed turn has been introduced the formation of other left-handed turns will be favored. It remains an open question whether residues preferring a right-handed α-helical conformation at the critical positions in a sequence that has exterior and interior residues exchanged would induce a structure with a right-handed β-helix but otherwise high structural similarity to Cam.

Structural evidence supporting a new class of carbonic anhydrases

The sequence alignment of putative proteins related to Cam (Figure 5) suggests that these proteins adopt the same fold of a left-handed β-helix as Cam. The strong type conservation of residues pointing into the interior of the β-helix and conservation of important Gly residues in β-turns support this hypothesis. Since all the His ligands to the Zn^{2+} and Gln75 are strictly conserved, it seems

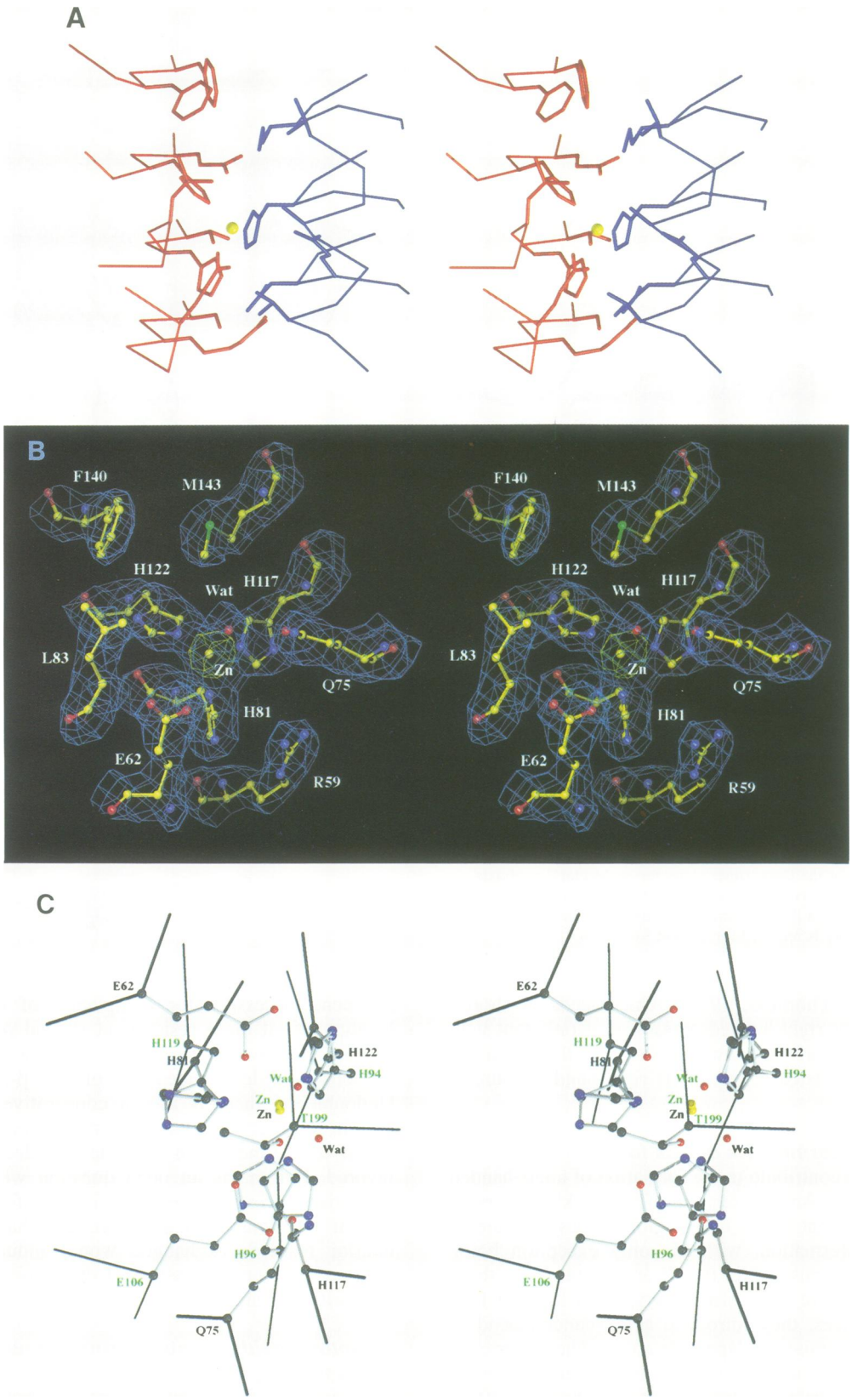

Fig. 4. (**A**) Active site view of Cam looking along the presumed pathway leading to the Zn^{2+} ion. Residues of one monomer are shown in red and residues of the second monomer in blue. (**B**) Electron density contoured at 1σ (blue) and 6σ (yellow) obtained after solvent flattening and 3-fold averaging around the Zn^{2+} ion. Gln75, His117 and Met135 belong to the second monomer. The putative water molecule at the fourth coordination site is labeled Wat. (**C**) Active site superposition of the Zn^{2+} ions and the coordinating His residues of Cam and CBAII. Short stretches of Cα trace are shown as thick and thin lines for Cam and CBAII, respectively. The side chains of residues involved in metal coordination or presumably enzymatic activity and the Zn^{2+}-bound water molecules (Wat) are shown in ball-and-stick representation and are labeled in black (Cam) or green (CBAII).

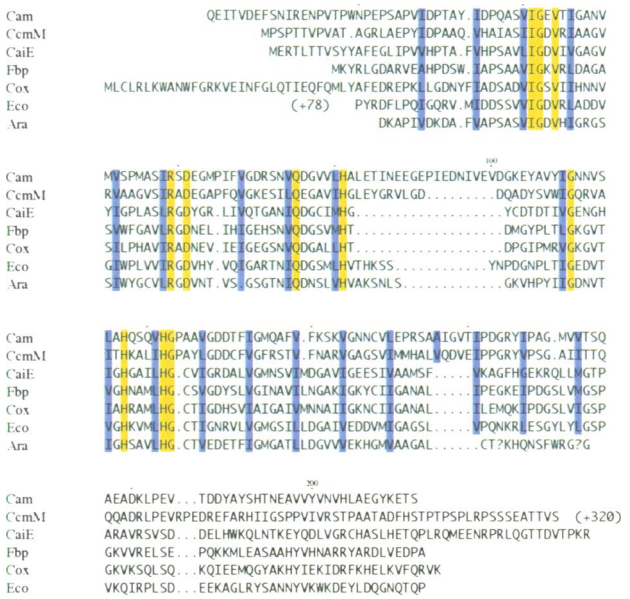

Fig. 5. Multiple sequence alignment of putative proteins sharing significant identity with Cam. Identical residues are highlighted in yellow, type-conserved aliphatic side chains pointing into the interior of the β-helix in blue, insertions are denoted by periods and every 20th residue is labeled by a dot. Abbreviations are CcmM for a putative CO_2 concentrating protein from *Synechococcus sp.*, CaiE for an open reading frame from *Escherichia coli*, Fbp for a ferripyochelin binding protein from *Pseudomonas aeruginosa*, Cox and Eco denote two open reading frames from *Coxiella burnetii* and *E.coli*, respectively (all these sequences were obtained from GenBank) and Ara represents a partial protein sequence deduced from an 'expressed sequence tag' of *Arabidopsis thaliana* (sequence obtained from the EST database). Uncertain residues in this sequence are identified by a ?. Numbers (+78 and +320) indicate extensions of the respective polypeptide by the specified number of residues.

plausible that not only the fold, including the trimeric architecture and location of the Zn^{2+} binding site at the interface of the two monomers, but also the function of these proteins is the same. Thus, the crystal structure defines Cam as the first member of the proposed new class of carbonic anhydrases (Alber and Ferry, 1994), a class that is present in all three phylogenetic domains of life: *Archaea*, *Bacteria* and *Eucarya*.

Materials and methods

Crystallization

Cam was heterologously produced in *Escherichia coli* excluding the putative signal sequence (B.E.Alber and J.G.Ferry, in preparation). The purified enzyme (17 mg/ml) was crystallized using 2.0 M $(NH_4)_2SO_4$/3% PEG400 as precipitant in 0.1 M cacodylate buffer, pH 6.5 and 0.02% NaN_3 yielding tetragonal crystals and using 30% PEG400 in 0.1 M HEPES buffer, pH 7.5, 0.2 M $MgCl_2$ and 0.02% NaN_3 yielding orthorhombic crystals. Crystals either belong to space group $P4_32_12$ with a = b = 71.84 Å and c = 333.51 Å with three molecules per asymmetric unit or to space group $P2_12_12_1$ with a = 67.22 Å, b = 70.40 Å and c = 311.07 Å containing six molecules in the asymmetric unit. Due to superior diffraction quality and reproducibility of the tetragonal crystals, they were used for structure solution by multiple isomorphous replacement.

Data collection

Native datasets for the tetragonal crystal form, as well as the PIP2 dataset were collected at room temperature on beam line 7.1 at the Stanford Synchrotron Radiation Laboratory (SSRL) with a MAR Research imaging plate detector at a wavelength of 1.08 Å. The remaining datasets were collected on an R-Axis IIC imaging plate using monochromatized CuK_α radiation produced by a Rigaku RU 200 rotating anode generator operating at 50 kV and 100 mA. The data were processed with DENZO (Otwinowski, 1993) and scaled with ROTAVATA/AGROVATA (Bailey, 1994). For all subsequent calculations, programs of the CCP4 suite (Bailey, 1994) were used, with exceptions as indicated.

Heavy atom derivatives and phase determination

Heavy atom derivatives were prepared by soaking crystals in mother liquor containing 0.5 mM di-μ-iodo-*bis*-(ethylenediamine) di-platinum II nitrate for 46 h (PIP1), 0.5 mM of the same compound for 84 h (PIP2), 0.75 mM $K[Au(CN)_2]$ for 56 h (AU) and 10 mM $(CH_3)_3PbAc$ for 5 days (PB). Heavy atom sites for the PIP derivative were determined by direct methods using SHELXS-86 (Sheldrick, 1990) and the other derivatives were solved by difference Fourier methods. Heavy atom parameters were refined and phases were calculated with MLPHARE (Otwinowski, 1991) at a resolution of 4 Å. The initial phases were improved by solvent flattening (solvent content of 50%) using SOLOMON (Abrahams and Leslie, 1996) resulting in a figure of merit (FOM) of 0.894. The map calculated with these improved phases revealed three molecules in the asymmetric unit related by a molecular 3-fold axis.

Three-fold electron density averaging

Initial ncs relationships were determined from the positions of equivalent skeleton atoms and improved using the Uppsala suite of averaging programs (Kleywegt and Jones, 1994) which was also used to produce masks for the three monomers. Averaging of the electron density maps and phase extension from 4 to 2.8 Å was carried out using SOLOMON against dataset NAT2. After the last cycle, the R-factor between the observed structure factor amplitudes and those calculated after inversion of the map was 0.188 with a FOM of 0.888. The resulting electron density map was of very good quality and showed as highest features the Zn^{2+} ions as well as continuous density for residues 0–212 (residue 0 corresponds to an additional methionine that is part of the protein after expression in *E.coli*) and an atomic model was built using O (Jones *et al.*, 1991).

Refinement

The structure has been refined at 2.8 Å resolution with the simulated annealing protocol in X-PLOR (Brünger, 1992) using the stereochemical parameters of Engh and Huber (1991) followed by restrained isotropic B-factor refinement. Very tight ncs restraints were incorporated in the refinement resulting in pairwise r.m.s. deviations below 0.05 Å for all atoms. The current model contains 4839 atoms in residues 0–212 of the three molecules, three Zn^{2+} ions and three water molecules. The last residue, Ser213, as well as the side chain of Glu22, is disordered in all three monomers. The crystallographic R-factor is 0.235 for all data (free R-factor of 0.293) and the stereochemistry of the model is very good with r.m.s deviations of 0.013 Å in bond lengths and 1.7° in bond angles. The structure has been analyzed with PROCHECK (Laskowski *et al.*, 1993) revealing that nine out of 10 parameters describing the quality of the model are better by at least one standard deviation than usually observed for structures at this resolution. For instance, 81.1% of all residues are in the most favored regions of the Ramachandran diagram and no residues are in disallowed regions.

Orthorhombic crystal form

The dataset of the orthorhombic form was 0.821 complete to 4 Å resolution (0.698 in the highest shell) with an R_{merge} of 0.154 (0.392). The structure of Cam in this crystal form was solved by molecular replacement using AMORE (Navaza, 1994) with the hexamer as a search model. A clear solution for the rotation and subsequent translation function was found which had an R-factor of 0.389 and a correlation coefficient of 0.671 using data between 15 and 5.5 Å. After rigid body refinement in X-PLOR, the R-factor dropped to 0.309 for data between 13 and 4 Å, refining the six monomers as individual rigid bodies. Due to the poor diffraction of these crystals, structure analysis is based on the model derived form the tetragonal crystal form.

Acknowledgements

The authors would like to thank Dr Joachim Behlke for carrying out the analytical ultracentrifugation experiments. This work was supported by Deutsche Forschungsgemeinschaft postdoctoral fellowships (to C.K. and H.S.), by USPHS and NSF grants (to D.C.R.) and by an NIH grant (to J.G.F.). The rotation camera facility at SSRL is supported by DOE and

NIH. Coordinates have been deposited in the Protein Data Bank PDBID code ITHJ, they can also be requested by E-mail to kisker@citray.caltech.edu.

References

Abrahams,J.P. and Leslie,A.G.W. (1996) Methods used in the structure determination of bovine mitochondrial F_1 ATPase. *Acta Crystallogr.*, **D52**, 30–42.

Ævarsson,A., Brazhnikov,E., Garber,M., Zheltonosova,J., Chirgadze,Y., Al-Karadaghi,S., Svensson,L.A. and Liljas,A. (1994) Three-dimensional structure of the ribosomal translocase: elongation factor G from *Thermus thermophilus*. *EMBO J.*, **13**, 3669–3677.

Alber,B.E. and Ferry,J.G. (1994) A carbonic anhydrase from the archaeon *Methanosarcina thermophila*. *Proc. Natl Acad. Sci. USA*, **91**, 6909–6913.

Bacon,D. and Anderson,W.F. (1988) A fast algorithm for rendering space-filling molecule pictures. *J. Mol. Graphics*, **6**, 219–220.

Bailey,S. (1994) The CCP4 suite—programs for protein crystallography. *Acta Crystallogr.*, **D50**, 760–763.

Bjorkman,P.J., Saper,M.A., Samaroui,B., Bennet,W.S., Strominger,J.L. and Wiley,D.C. (1987) Structure of the human class I histocompatibility antigen, HLA-A2. *Nature*, **329**, 506–512.

Brünger,A.T. (1992) *X-PLOR Version 3.1—A System for X-ray Crystallography and NMR*. Yale University Press, New Haven and London.

Engh,R.A. and Huber,R. (1991) Accurate bond and angle parameters for X-ray protein-structure refinement. *Acta Crystallogr.*, **A47**, 392–400.

Fukuzawa,H., Suzuki,E., Komukai,Y. and Miyachi,S. (1992) A gene homologous to chloroplast carbonic anhydrase (*icfA*) is essential to photosynthetic carbon dioxide fixation by *Synechococcus* PCC7942. *Proc. Natl Acad. Sci. USA*, **89**, 4437–4441.

Gu,F., Khimani,A., Rane,S.G., Flurkey,W.H., Bozarth,R.F. and Smith,T.J. (1995) Structure and function of a virally encoded fungal toxin from *Ustilago maydis*: a fungal and mammalian Ca^{2+} channel inhibitor. *Structure*, **3**, 805–814.

Håkansson,K., Carlsson,M., Svensson,L.A. and Liljas,A. (1992) Structure of native and apo carbonic anhydrase II and structure of some of its anion–ligand complexes. *J. Mol. Biol.*, **227**, 1192–1204.

Jones,T.A., Zou,J.Y., Cowan,S.W. and Kjeldgaard,M. (1991) Improved methods for building protein models in electron density maps and the location of errors in these models. *Acta Crystallogr.*, **A47**, 110–119.

Kleywegt,G.J. and Jones,T.A. (1994) Halloween . . . masks and bones. In Bailey,S., Hubbard,R. and Waller,D.A. (eds), *From First Map to Final Model*. SERC Daresbury Laboratory, UK, pp. 59–66.

Kraulis,P.J. (1991) MOLSCRIPT—a program to produce both detailed and schematic plots of protein structures. *J. Appl. Crystallogr.*, **24**, 946–950.

Laskowski,R.A., Mcarthur,M.W., Moss,D.S. and Thornton,J.M. (1993) PROCHECK—a program to check the stereochemical quality of protein structures. *J. Appl. Crystallogr.*, **26**, 283–291.

Lietzke,S.E., Keen,N.T., Yoder,M.D. and Jurnak,F. (1994) The three-dimensional structure of pectate lyase E, a plant virulence factor from *Erwinia chrysanthemi*. *Plant Physiol.*, **106**, 849–862.

Lindskog,S. (1983) Carbonic anhydrase. In Spiro,T.G. (ed.), *Zinc Enzymes*. John Wiley & Sons, New York, Vol. 5, pp. 77–121.

Navaza,J. (1994) AMORE—an automated package for molecular replacement. *Acta Crystallogr.*, **A50**, 157–163.

Otwinowski,Z. (1991) Maximum likelihood refinement of heavy atom parameters. In Wolf,W., Evans,P. and Leslie,A. (eds), *Isomorphous Replacement and Anomalous Scattering*. SERC Daresbury Laboratory, UK, pp. 80–86.

Otwinowski,Z. (1993) Oscillation data reduction program. In Sawyer,L., Isaacs,N. and Bailey,S. (eds), *Data Collection and Processing*. SERC Daresbury Laboratory, UK, pp. 56–62.

Pickersgill,P., Jenkins,J., Harris,G., Nasser,W. and Robert-Baudouy,J. (1994) The structure of *Bacillus subtilis* pectate lyase in complex with calcium. *Nature Struct. Biol.*, **1**, 717–723.

Raetz,C.R.H. and Roderick,S.L. (1995) A left-handed parallel β helix in the structure of UDP-*N*-acetylglucosamine acyltransferase. *Science*, **270**, 997–1000.

Richardson,J.S. (1976) Handedness of crossover connections in β sheets. *Proc. Natl Acad. Sci. USA*, **73**, 2619–2623.

Schulz,G.E. and Schirmer,R.H. (1979) *Principles of Protein Structure*. Springer Verlag, Heidelberg.

Sheldrick,G.M. (1990) Phase annealing in SHELX-90—direct methods for larger structures. *Acta Crystallogr.*, **A46**, 467–473.

Sly,W.S. and Hu,P.Y. (1995) Human carbonic anhydrases and carbonic anhydrase deficiencies. *Annu. Rev. Biochem.*, **64**, 375–401.

Steinbacher,S., Seckler,R., Miller,S., Steipe,B., Huber,R. and Reinemer,P. (1994) Crystal structure of P22 tailspike protein: interdigitated subunits in a thermostable trimer. *Science*, **265**, 383–386.

Sternberg,M.J.E. and Thornton,J.M. (1977) On the conformation of proteins: the handedness of the connection between parallel β-strands. *J. Mol. Biol.*, **110**, 269–283.

Wilmot,C.M. and Thornton,J.M. (1988) Analysis and prediction of the different types of β-turns in proteins. *J. Mol. Biol.*, **203**, 221–232.

Wright,C.S., Alden,A.R.A. and Kraut,J. (1969) Structure of subtilisin BPN′ at 2.5 Å resolution. *Nature*, **221**, 235–242.

Xue,Y., Liljas,A., Jonsson,B.-H. and Lindskog,S. (1993) Structural analysis of the zinc hydroxide–Thr-199–Glu-106 hydrogen-bond network in human carbonic anhydrase II. *Proteins: Struct. Funct. Genet.*, **17**, 93–106.

Yoder,M.D. and Jurnak,F. (1995) The parallel β helix and other coiled folds. *FASEB J.*, **9**, 335–342.

Yoder,M.D., Keen,N.T. and Jurnak,F. (1993) New domain motif: the structure of pectate lyase C, a secreted plant virulence factor. *Science*, **260**, 1503–1507.

Received on November 17, 1995; revised on January 9, 1996